Picosecond dynamics of excitons in cubic GaN

R. Klann, O. Brandt, H. Yang, H. T. Grahn, and K. Ploog

Paul-Drude-Institut für Festkörperelektronik, Hausvogteiplatz 5-7, D-10117 Berlin, Germany

A. Trampert

Max-Planck-Institut für Festkörperforschung, Heisenbergstrasse 1, D-70569 Stuttgart, Germany

(Received 8 June 1995; revised manuscript received 28 July 1995)

Using time-resolved photoluminescence, we investigate the spectral and temporal behavior of the near-band-edge emission located at 3.255–3.27 eV of cubic GaN/GaAs(001) grown by plasma-assisted molecular-beam epitaxy. In contrast to transitions at lower energies, this narrow high-energy emission band exhibits an ultrafast dynamics on a picosecond time scale. The decay is characterized by a biexponential behavior composed of a fast initial component (15–40 ps) followed by a second, slower component (100–400 ps). We attribute the initial decay to radiative decay of free excitons and the relaxation towards bound states. The second slower component is assigned to the radiative recombination of these bound excitons. This interpretation is supported by intensity-dependent measurements.

Recently, the interest in GaN and related compounds has increased dramatically by the demonstration of high-brightness light emitting diodes in the blue spectral region.[1] The spontaneous emission employed for these devices originates from donor-acceptor transitions provoked by intentional codoping of the active region.[2] The quest for a blue laser based on this material system, however, has to follow a different path, since stimulated emission in semiconductors arises not from impurity, but from band-to-band or exciton transitions. An essential prerequisite for such devices is the knowledge of the band structure as well as an insight into carrier relaxation and recombination processes. For cubic GaN, however, the situation is such that even the band gap is still a matter of controversy.[3,4]

For the sake of fundamental studies, we have grown samples under conditions giving rise to large, undoubtedly cubic GaN single crystals as judged by their *habitus* and by transmission electron diffraction (TED) patterns. These crystals exhibit intense and narrow photoluminescence (PL) lines spectrally located between 3.0 and 3.27 eV, which allows the investigation of carrier relaxation and recombination processes by time-resolved spectroscopy.

In this paper, we present the transient photoluminescence for two different samples labeled A and B, whose PL spectra are dominated by the emission of these crystals. Although the average crystals' sizes for samples A and B are very different, the transient PL behavior is found to be quite the same, suggesting that the decay characteristics observed are an intrinsic property. Here, we concentrate on the highest energy line in both samples. At 5 K, the decay of this line is biexponential with an ultrafast initial time constant (15–40 ps) and a second, slower component (100–400 ps).

The samples under investigation are grown by solid-source molecular-beam epitaxy, employing a dc plasma discharge source for dissociating molecular N_2 into activated nitrogen species. GaAs(001) is used as substrate. Growth of GaN is initiated at 630–680 °C under near stoichiometric conditions using a slow growth rate (0.05 ML/s).

After establishing a smooth, cubic GaN layer as revealed by reflection high-energy electron diffraction, the Ga flux is increased by a factor of 4. Ga droplets are then formed on the growth front, giving rise to a vapor-liquid-solid-like growth of cubic GaN crystals inside the droplets. After growth is completed, the samples are treated with concentrated HCl which removes liquid Ga and thus allows the access of the GaN crystals on the surface. For the present samples, these crystals exhibit smooth facets characteristic of the zinc-blende structure and are of average sizes of 3 μm (sample A) and 0.3 μm (sample B). Figure 1 shows the TED patterns of sample B taken from the cubic GaN crystals (a) and from the surrounding GaN film (b). Both patterns reveal the symmetry of the zinc-blende structure. The film exhibits a high density of stacking faults as evidenced by the streaks connecting the Bragg spots along the $\langle 111 \rangle$ directions. These streaks are virtually absent in the patterns from the cubic GaN crystal, demonstrating their single-crystal nature.

Time-resolved PL measurements are performed using a femtosecond Ti:sapphire laser and a syncroscan streak-camera system. The 150-fs pulses with a repetition rate of 76
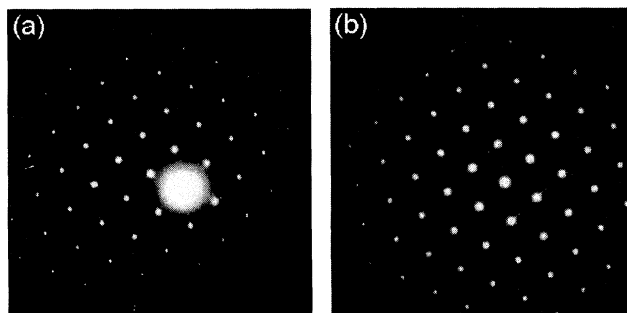
FIG. 1. Transmission electron diffraction patterns taken from sample B. In (a), the pattern from a cubic GaN single crystal is displayed, while (b) is taken from the surrounding GaN film. Note the absence of stacking-fault streaks in pattern (a).
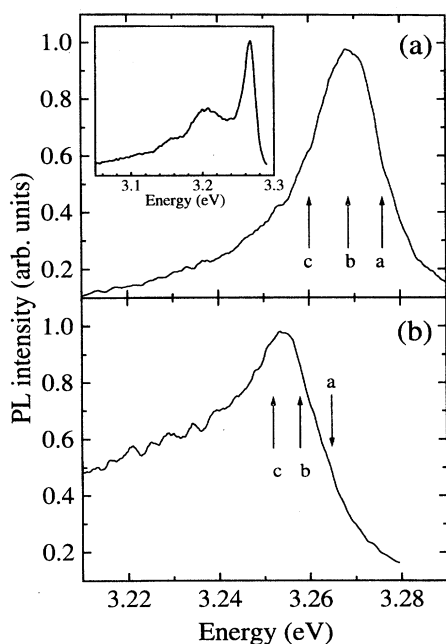
FIG. 2. Time-resolved PL spectra at 5 K for the two samples A (a) and B (b) with E_{ex} = 3.36 eV averaged over 100 ps after excitation. The arrows labeled a, b, and c indicate the energy positions of the transients in Fig. 3. The inset shows the cw PL spectrum for sample A.

MHz are frequency doubled allowing us to tune the excitation from 3.10 to 3.40 eV (full width at half maximum 20 meV). If not stated otherwise, the excitation power is set to 60 μW, which corresponds to a peak power density of 5
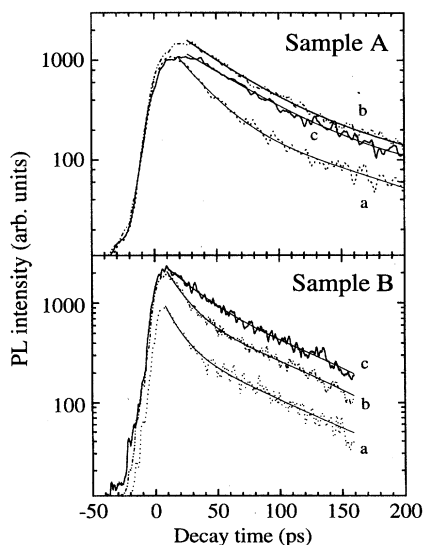
FIG. 3. Transient PL decay at 5 K for the two samples A and B during the first 150 ps after excitation with E_{ex} = 3.36 eV. The three energy positions a (dotted line), b (dash-dotted line), and c (full line) are indicated in Fig. 2 (spectrally averaged over 5 meV). The solid lines are least-square fits to the data using a biexponential.

TABLE I. Fast (τ_f) and slow (τ_s) time constants for samples A and B as derived from a biexponential fit to the transients a, b, and c in Fig. 3.

	Sample A			Sample B		
	a	b	c	a	b	c
τ_f (ps)	30	40	40	15	35	40
τ_s (ps)	100	313	280	214	320	400

kW/cm^2 (fluence 7.5 nJ/cm^2). The luminescence is dispersed by a 22-cm monochromator using a 1200-lines/mm grating and focused onto the photocathode of the streak tube. The spectral resolution amounts to 0.4 nm; the temporal resolution is 2 ps. The samples are mounted on the cold finger of a He flow cryostat and kept at 5 K.

The inset in Fig. 2 shows the cw PL spectrum for sample A. An intense line is found at 3.27 eV. The weaker lines down to 3.1 eV, which apparently are impurity-related transitions, exhibit a delayed rise of several hundreds of picoseconds and decay on a time scale of several tens of nanoseconds. In the following we will focus on the peak highest in energy. Transient PL spectra at 5 K averaged over the first 100 ps are shown in Fig. 2 for an excitation energy of 3.36 eV. For sample A [Fig. 2(a)] the spectrum is dominated by an asymmetric sharp line at 3.27 eV. The corresponding peak for sample B [Fig. 2(b)] appears at 3.255 eV. It is broader resulting from the more pronounced shoulder at the low-energy side. The spectral shift of 15 meV between these peaks and the different contribution of the low-energy broadening is due to the different sample quality and will be discussed later. We found no change in the PL intensity by tuning the excitation energy from 3.30 to 3.40 eV. Therefore, we conclude that the band-gap energy of cubic GaN is below 3.32 eV.

The picosecond dynamics of the peaks is visualized in Fig. 3. The energy positions of the three transients for each sample are marked by the arrows a, b, and c in Fig. 2. For all spectral positions and both samples the PL rise time is below 5 ps, i.e., of the order of our time resolution. The PL
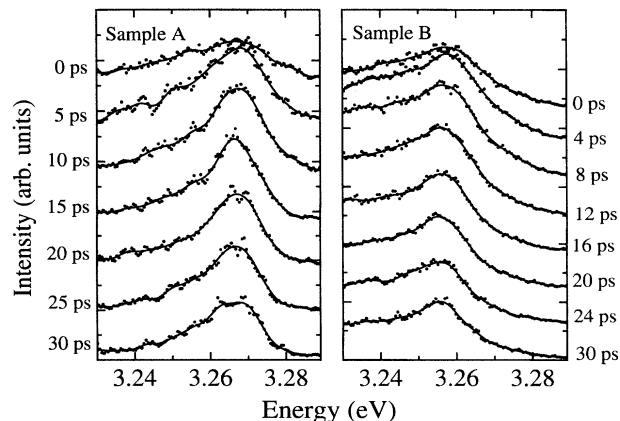
FIG. 4. Transient PL spectra for samples A and B for different decay times as indicated (spectral average over 2 ps). The spectra have been shifted vertically. The lines are a guide to the eye.
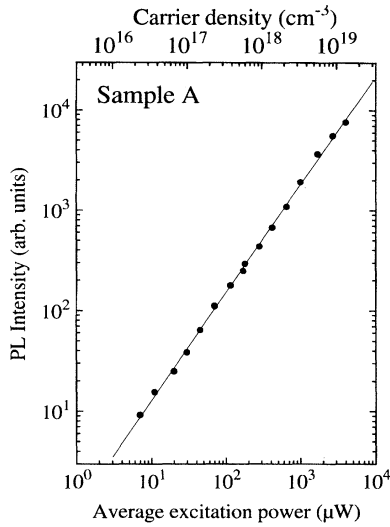
FIG. 5. Integrated PL intensity of the peak at 3.268 eV in the transient spectrum of sample A vs excitation power (dots). The carrier density was estimated by the photon flux, the calculated absorption coefficient, and the carrier lifetime. The full line is the linear regression of the data points with a slope of 1.

decay behavior is biexponential with a first fast time constant τ_f of 15 to 40 ps depending on the spectral position. This first decay component is faster for both samples on the high-energy side (transients a) than on the lower-energy side (transients c). For sample A the transients lower in energy (b and c) show even a delayed onset of the decay compared to transient a which is detected at higher energies. The second slower time constant τ_s ranges from 100 to 400 ps. The time constants derived from our data by a least-square fit to a biexponential are compiled in Table I. The spectral evolution during the first 30 ps is plotted in Fig. 4. At very early times the line is broad, particularly on the high-energy side. With increasing time delay, the spectra become steeper on the high-energy side and the PL maxima shift about 5 meV to lower energies for both samples.

The integrated intensity of the high-energy PL peak at 3.27 eV from the time-resolved spectra of sample A (see Fig. 2) vs average excitation power is displayed in Fig. 5 (dots). A strictly linear dependence over three orders of magnitude is found up to very high densities (line). This linear dependence demonstrates that no nonradiative decay channels participate in the decay process for this power range.[5] The same linear behavior is found in cw spectra for lower excitation levels. The average carrier density n given at the top axis of Fig. 5 was estimated by the incident photon flux ϕ, the calculated absorption coefficient α and the measured carrier lifetime τ.[6]

The linear dependence of the PL intensity on excitation density up to carrier concentrations of 10^{19} cm^{-3} is consistent with both band-to-band and excitonic transitions, but not with impurity-related transitions. The observed ultrafast biexponential decay is independent on excitation density and thus cannot arise from band-to-band transitions, but must be excitonic [note the low excitation density ($\approx 10^{17}$ cm^{-3}) used for the experiments shown above]. This conclusion is furthermore supported by the temperature dependence of the spectral position of the PL line, which follows the temperature behavior for the band gap of cubic GaN as reported by Ramírez-Flores et al.[3] with a constant offset of 25 meV up to room temperature.[7] Because of its spectral width, the PL line presumably consists of a spectrally unresolved superposition of the radiative transitions of both free and bound excitons. Only the pronounced broadening of the spectra at $t = 0$ ps (Fig. 4) may arise from the onset of electron-hole plasma emission (the excess energy per excitation photon is about 60 meV). We attribute the initial fast decay component (τ_f) to the free exciton decay rate, which is composed of both the radiative decay and the relaxation of the exciton towards localized states. The second, slower decay component (τ_s) is attributed to the radiative decay of these localized exciton states. For the high-quality sample A the peak at 3.27 eV originates mainly from free excitons, whereas the bound excitons which are lower in energy contribute only weakly to the PL emission. In contrast, the spectra of sample B are dominated by localized excitons as evidenced by the spectral shift of 15 meV to lower energies for this sample.

The radiative lifetime of bound and localized excitons[8] is given in first order by

$$\tau_r = \frac{3 \pi m_0^2 \hbar c_0^3 \epsilon_0}{\bar{n} \omega e^2 |p_{cv}|^2}, \tag{1}$$

where the symbols have the same meaning as given in Ref. 6. This equation predicts a radiative lifetime on the order of 400 ps for bound and localized excitons in GaN, which is in close agreement with our results. Note that this value is shorter than in, e.g., GaAs primarily because of the different band gaps. At present, we cannot decide whether the localizing states are provided by native defects, impurities, or crystal disorder. However, findings similar to ours in various II-VI and III-V semiconductors[9–12] have been interpreted by disorder-induced localization of excitons. In fact, the spectral redshift within the first 30 ps (see Fig. 4), the dependence of the PL transients on the energy position in the PL line, as well as the delayed onset of the PL decay for transient c in Fig. 3 are all consistent with this picture.

In conclusion, we have investigated the picosecond dynamics of the PL line highest in energy in cubic GaN in different samples. The PL signal, which rises within our time resolution, shows a biexponential decay behavior. The fast PL decay component of 15 to 40 ps is attributed to the radiative decay and relaxation of free excitons. The slower PL decay component of 100 to 400 ps is attributed to the recombination of localized excitons. The band-gap energy of cubic GaN is estimated from these results to be 3.29 ±0.01 eV.

[1] S. Nakamura, T. Mukai, and M. Senoh, Appl. Phys. Lett. **64**, 1687 (1994).

[2] S. Nakamura, T. Mukai, and M. Senoh, J. Appl. Phys. **76**, 8189 (1994); S.D. Lester, F.A. Ponce, M.G. Craford, and D.A. Steigerwald, Appl. Phys. Lett. **66**, 1249 (1995).

[3] G. Ramírez-Flores, H. Navarro-Contreras, A. Lastras-Martínez, R.C. Powell, and J.E. Greene, Phys. Rev. B **50**, 8433 (1994).

[4] C.H. Hong, D. Pavlidis, S.W. Brown, and S.C. Rand, J. Appl. Phys. **77**, 1705 (1995).

[5] T. Schmidt, K. Lischka, and W. Zulehner, Phys. Rev. B **45**, 8989 (1992).

[6] Since excitation is not resonant to the exciton state, but takes place in the continuum above the band gap E_G (3.3 eV), the carrier density n is given by $n = \alpha \phi \tau$, where

$$\alpha = \frac{e^2}{\tilde{n} m_0^2 \omega c_0 \epsilon_0} \left(\frac{2\mu}{\hbar^2}\right)^{\frac{3}{2}} \frac{|p_{cv}|^2}{1-e^{-2\gamma}} \Theta(\hbar\omega - E_G)\sqrt{E_x},$$

with $\gamma = \pi\sqrt{E_x/(\hbar\omega - E_G)}$ [E_x exciton binding energy (25 meV), $\tilde{n}$ refractive index (2.5), e electron charge, $\hbar\omega$ excitation energy (3.36 eV), p_{cv} momentum matrix element ($2|p_{cv}|^2/m_0 \simeq 22$ eV), μ reduced mass ($1/\mu = 1/m_c + 1/m_v$ with $m_c = 0.2 m_0$ and $m_v = 0.4 m_0$), m_0 electron mass, c_0 speed of light, ϵ_0 dielectric constant].

[7] J. Mäuser, O. Brandt, H. Yang, and K. Ploog (unpublished).

[8] É.I. Rashba, Fiz. Tekh. Poluprovodn. **8**, 1241 (1974) [Sov. Phys. Semicond. **8**, 807 (1975)]; C.J. Hwang and L.R. Dawson, Solid State Commun. **10**, 443 (1972).

[9] J.A. Kash, A. Ron, and E. Cohen, Phys. Rev. B **28**, 6147 (1983).

[10] J.A. Kash, Phys. Rev. B **29**, 7069 (1984).

[11] E.F. Schubert and W.T. Tsang, Phys. Rev. B **34**, 2991 (1986).

[12] S. Shevel, R. Fischer, E.O. Göbel, G. Noll, P. Thomas, and C. Klingshirn, J. Lumin. **37**, 45 (1987).

FIG. 1. Transmission electron diffraction patterns taken from sample B. In (a), the pattern from a cubic GaN single crystal is displayed, while (b) is taken from the surrounding GaN film. Note the absence of stacking-fault streaks in pattern (a).